Current Journal of Applied Science and Technology

40(21): 25-31, 2021; Article no.CJAST.73180
ISSN: 2457-1024
(Past name: British Journal of Applied Science & Technology, Past ISSN: 2231-0843, NLM ID: 101664541)

Analysis of Versions of the RX Algorithm for Anomaly Detection in Hyperspectral Images

Chinmayee Dora[1*] and Jharna Majumdar[1]

[1]School of Engineering & Technology (SoET), Centurion University of Technology & Management, India.

Authors' contributions

This work was carried out in collaboration between both authors. Both authors read and approved the final manuscript.

Article Information

DOI: 10.9734/CJAST/2021/v40i2131468
Editor(s):
(1) Ming-Chih Shih, Chinese Culture University, China.
Reviewers:
(1) M Pradeep, India.
(2) Mário P. Véstias, Portugal.
Complete Peer review History: https://www.sdiarticle4.com/review-history/73180

Short Communication

Received 22 June 2021
Accepted 02 September 2021
Published 03 September 2021

ABSTRACT

Anomaly Detection with Hyper Spectral Image (HSI) refers to finding a significant difference between the background and the anomalous pixels present in the image. This paper offers a study on the Reed Xiaoli Anomaly (RXA) detection algorithm performance investigated for increasing number of spectral bands from 30, 50, 100 to all the spectral bands present in the HSI. The original RXA algorithm is formulated with Mahalanobis distance. In this study the RXA al is re-implemented with other different distance algorithms like Bhattacharya distance, Kullback-Leibler divergence, and Jeffery divergence and evaluated for any change in the performance. For the first part of investigation, the obtained results showed that the decreased number of spectral bands shows better performance in terms of receiver operating characteristic (ROC) obtained for cumulative probability values and false alarm rate. In the next part of study it is found that, the RXA algorithm with Jeffrey divergence has a comparable performance in ROC to that of the RX algorithm with Mahalanobis distance.

Keywords: Hyperspectral image; RX algorithm; Mahalanobis distance; Bhattacharya distance; Kullback-Leibler divergence; Jeffery divergence.

**Corresponding author: E-mail: chinmayee@cutm.ac.in;*

1. INTRODUCTION

Anomaly detection is to detect objects that are not similar to the predicted pattern of the data. For images, it refers to the detection of pixels showing a different spectral signature in comparison to the pixels in an image. Image anomaly detection is one of the most fascinating and critical tasks for many upper-level image- and video-based applications, e.g., surveillance, environmental monitoring, and medical analysis [1,2].

Reed-Xiaoli detector often called RX detector for short, is one of the extensively used validated techniques for anomaly detection [3], which is the widely used example of anomaly detectors basing on covariance. This type of detectors has broad uses in many domains, from hyperspectral images (HSI) to medical images [4]. The anomaly detection work can be divided into two sub-problems: how to define the background (BG) and how to calculate the anomaly numerically. RX detector assumes that the BG is relatively similar and models it with a multivariate Gaussian distribution. But it may happen that this assumption could not always be sufficient. Hence, several variations to RXA are investigated in this paper with respect to these two sub-problems. In this paper, five variations of RXA compared in terms of accuracy on real HSI datasets. Also, in this paper the number of band selected is restricted to 30 and studied the impact of number of increasing bands on the results obtained.

The paper is organised as follows: First a brief introduction to RXA detector is given in section 2. Then the proposed study is presented in Section 3. The performance of the proposed study evaluated and compared with those by the conventional RX algorithm both visually and objectively in Section 4 along with the dataset used. Finally, conclusion is drawn in Section 5.

2. REED-XIAOLI DETECTION ALGORITHM

RX detection algorithm by Reed and Yu is the most widely known and employed algorithm for anomaly detection and been used as a standard algorithm for many anomaly detection problems [5,6,7,8]. RXA detection algorithm assumes that the BG could be defined by using non-stationary multivariate Gaussian model and it is calculated by the image vector mean and covariance. It estimates the squared Mahalanobis separation by Mahalanobis [9] of each pixel from the estimated BG model. Pixels showing separation values over a defined threshold are assessed to be anomalous.

Mathematically, RX algorithm could be defined considering an HSI $\boldsymbol{I = [x_1; x_2; \ldots; x_{\mathbb{N}}]}$ which consists of $\mathbb{N}$ pixels, where the column vector $\boldsymbol{x_i = [x_{i1}; x_{i2}; \ldots; x_{im}]^T}$ presents the value of the *i-th* pixel over the *L* spectral bands of *I*. The assumed behaviour of BG pixels can be captivated by the mean vector μ_{mean} and covariance matrix C_B, are calculated as follows:

$$\mu_{mean} = \frac{1}{\mathbb{N}}\sum_{i=1}^{\mathbb{N}} x_i \; and \; C_B = \frac{1}{\mathbb{N}}\sum_{i=1}^{\mathbb{N}} \bar{x}_i \bar{x}_i^T$$

Where, $\bar{x}_i = (x_i - \mu_{mean})$, Mean vector and covariance matrix are calculated under the presumption that vectors $\boldsymbol{x}_i$ belongs to the same arbitary process; hence it could be assumed that anomaly is minor enough to have a non-significant impact on the calculated output [10].

Then, the generalized likelihood for anomaly of the pixel $\boldsymbol{x}$ w.r.t. the model $\boldsymbol{C_B}$ in terms of the square of the Mahalanobis distance [9], is expressed as:

$$D_{rxdm} = \bar{x}_i^T C_B^{-1} \bar{x}_i$$

Where, $C_B^{-1} = inverse(C_B)$, the inverse of the covariance matrix, also known as the precision matrix.

A decision threshold $\boldsymbol{v}$ is used to accept or reject the anomaly hypothesis. A general method is to set v adaptively as a percentage of $\boldsymbol{D_{rxdm}}$ changing range as follows:

$$\gamma = \delta . \max_{i=1,2,..,N} D_{rxdm}(x)$$

With δ limiting between (0,1). Then, if $\boldsymbol{D_{rxdm}(x) \geq v}$ the $\boldsymbol{x}$ is anomaly pixel.

3. PROPOSED VARIATIONS TO THE RX ALGORITHM

In this paper, instead of squared Mahalanobis distance in the RX algorithm, different distance formula are used to investigate and analyse the results for anomaly detection. The distance formulas investigated are: Bhattacharya distance, Kullback-Leibler (KL) distance, and Jeffery divergence.

3.1 Bhattacharya Distance

The Bhattacharya distance has been used as a class separability measure for different applications [11]. For two normally distributed classes, it is defined as follows:

$$D_{rxdb} = \frac{1}{8}(\mu_2 - \mu_1)^T \left[\frac{C_1}{C_2}\right]^{-1} (\mu_2 - \mu_1) + \frac{1}{2}\ln\frac{|C_1 + C_2/2|}{|C_1|^{\frac{1}{2}}|C_2|^{\frac{1}{2}}}$$

Where, ***μ*** and ***C*** are the mean vector and covariance matrix of the corresponding class, respectively. Here, the first class is each pixel vector present in the HS image and the second class is mean vector of all the pixel vector of the image.

3.2 Kullbeck-Leibler Divergence

The Kullback-Leibler divergence [12] is in close relation to the relative entropy, information divergence, and information for bias, is a non-symmetric to compute of the separation between two probability distributions ***p(x)*** and ***q(x)***. Specifically, the K-L divergence of ***q(x)*** from ***p(x)***, denoted D_{rxdKL}, is an estimate of the separation when ***q(x)*** is used for approximation of ***p(x)***. Let ***p(x)*** is the probability distributions of the pixel vector ***x*** and ***q(x)*** is the probability distributions of the means of the pixel vectors of the HSI. That is, both ***p(x)*** and ***q(x)*** sum up to 1, and $p(x) > 0$ and $q(x) > 0$ for any ***x*** in ***X***. Mathematically, D_{rxdKL} could be written as:

$$D_{rxdKL} = \sum_{x \in X} p(x) \ln \frac{p(x)}{q(x)}$$

3.3 Jeffery Divergence

The analytically derived Jeffrey divergence is an alteration of the K-L divergence which is stable, symmetric and robust w.r.t. noise and the volume of histogram bins [13]. It could be expressed as:

$$D_{rxdJ} = \sum \left(p(x) \log \frac{p(x)}{m(x)} + q(x) \log \frac{q(x)}{m(x)} \right)$$

Where, $m(x) = \frac{p(x)+q(x)}{2}$ and ***p(x)***, ***q(x)*** are as defined in the equation. This distance calculates how improbable it is that one distribution was derived from the population represented by the other.

4 RESULTS AND ANALYSIS

In this study, several real HS images are used. They are described below.

4.1 Dataset

- **Urban:** This is the most frequently used HS data used in the HS study. Originally, there are 307x307 pixels, each of which states a 2x2m^2 area. In this data, 210 wavelengths ranging from 400 nm to 2500 nm are present, which gives spectral resolution of 10 nm. Again, for this study, two subsets of the image are used here for anomaly detection which consists of 204 bands each with 100x100 pixels each.

- **Salinas scene:** This data image was gathered by the 224-band AVIRIS sensor over Salinas Valley, California, and has a high spatial resolution (3.7-meter pixels). The area covered spans 512´217. A subset of the image is used here for anomaly detection which consists of 204 bands each with 150x200 pixels.

- **PolSAR UAVSAR Images**: Two pairs of single-look quad-polarimetric SAR images captured by the UAVSAR airborne sensor in L-band over a town area in San Francisco city, are used for the experiments. It consists of two datasets, the dataset-1 have length and width of 200 pixels and the dataset-2 length and width of 100 pixels.

4.2 Implementation Results and Analysis

The implementation of the original RX algorithm and its variations are done using MATLAB R2018b. Here, 30 spectral bands are chosen for anomaly detection from the test HSI images. The study by Sun et al. [14] concluded that 20 to 30 spectral bands are sufficient for the anomaly detection. The results of band selection on the performance of the algorithm are shown using receiver operating characteristic (ROC) [15] in the Fig. 1. This ROC curve is for cumulative probability of distribution vs false alarm rate is shown for 30, 50, 100 and all the spectral bands considered for the RX anomaly detection algorithm. The ROC shows a better performance is obtained when only 30 bands are considered where the false alarm rate is getting restricted.

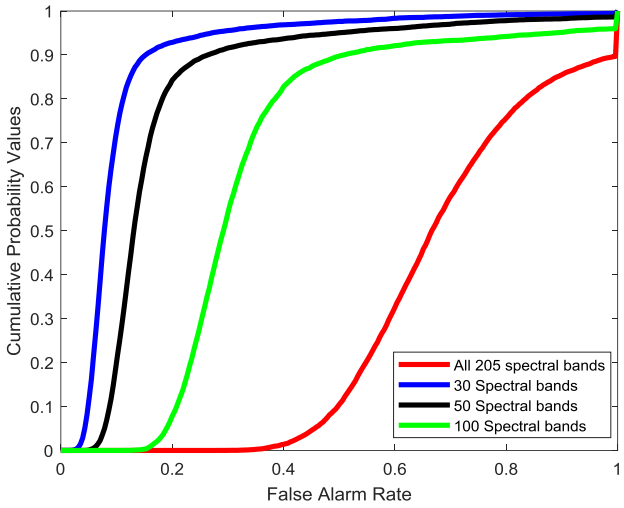

Fig. 1. ROC for different number of bands for anomaly detection using RX algorithm

The graphical results for the variation in RX algorithm with different distance measurement are shown in from Fig. 2 to Fig. 6 for different HS image dataset. As the graphical results shows, the RX algorithm with Bhattacharya distance is the lowest performing algorithm.

As the graphical results of RX algorithm with Bhattacharya distance has shown a lot of false alarms, the ROC of the same is eliminated from the results. Further, the ROC for the performance of the rest of the are algorithms plotted and shown in the Fig. 7. The ROC of RX algorithm with Mahalanobis distance and Jeffrey distance shows comparable results, whereas RX algorithm with KL distance shows declined performance for all the dataset.

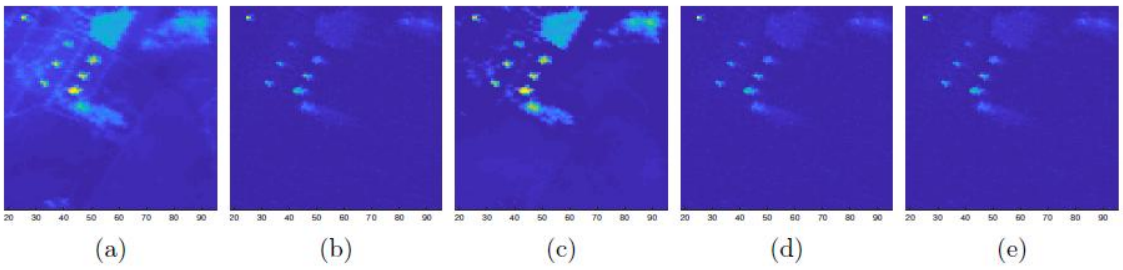

Fig. 2. (a) Original `Urban-1' Image, (b) RX algorithm with Mahalanobis distance, (c) RX algorithm with Bhattacharya distance, (d) RX algorithm with KL divergence, (e) RX algorithm with Jeffery divergence

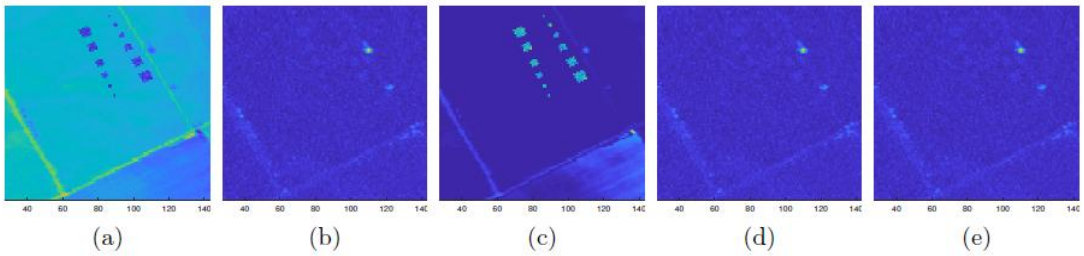

Fig. 3. (a) Original `Urban-2' Image, (b) RX algorithm with Mahalanobis distance, (c) RX algorithm with Bhattacharya distance, (d) RX algorithm with KL divergence, (e) RX algorithm with Jeffery divergence

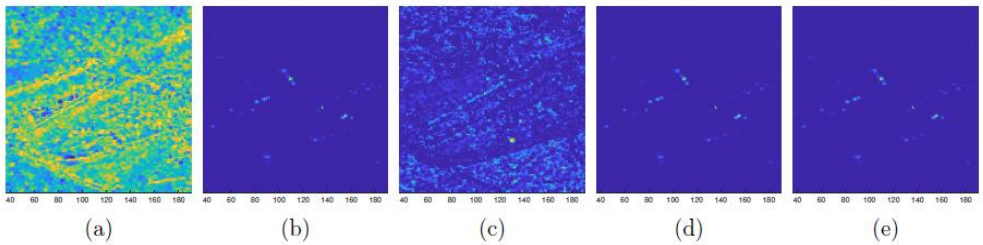

Fig. 4. (a) Original `Salinas' Image, (b) RX algorithm with Mahalanobis distance, (c) RX algorithm with Bhattacharya distance, (d) RX algorithm with KL divergence, (e) RX algorithm with Jeffery divergence

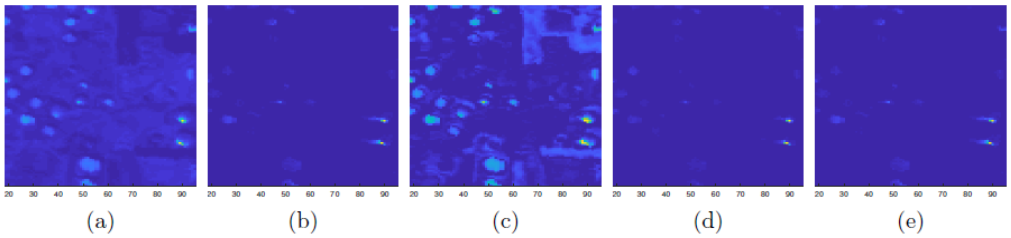

Fig. 5. (a) Original `Salinas' Image, (b) RX algorithm with Mahalanobis distance, (c) RX algorithm with Bhattacharya distance, (d) RX algorithm with KL divergence, (e) RX algorithm with Jeffery divergence

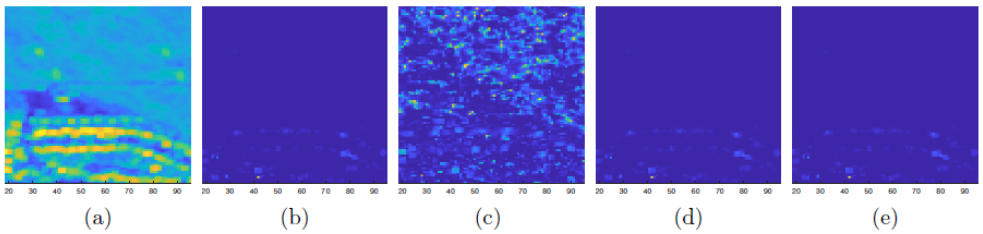

Fig. 6. (a) Original `Salinas' Image, (b) RX algorithm with Mahalanobis distance, (c) RX algorithm with Bhattacharya distance, (d) RX algorithm with KL divergence, (e) RX algorithm with Jeffery divergence

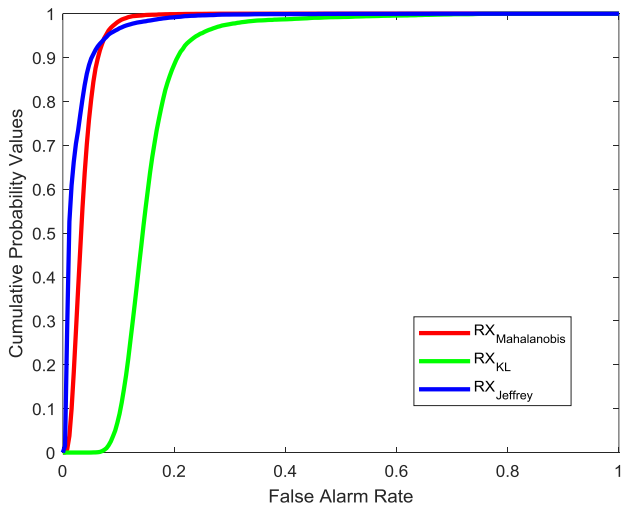

Fig. 7. ROC curves of the anomaly detectors with different distance formulas

5. CONCLUSION

In this paper, for the anomaly detection from HS images the original RX algorithm with Mahalanobis algorithm was implemented using different distance algorithms i.e., Bhattacharya distance, KL divergence, Jeffrey divergence. Also, the algorithm's anomaly detection performance is also investigated for number of spectral bands of HS image selected for the anomaly detection. It was found, when anomaly detection algorithm implemented with lower numbers of spectral bands of HS image, gave better ROC performance curve. Further, when performance ROC for the different variations of RX algorithm is investigated, RX algorithm with Mahalanobis distance and Jeffrey divergence gave comparable result while RX algorithm with KL divergence gave declined result.

ACKNOWLEDGEMENT

The authors express their sincere gratitude to Prof. Supriya Patnaik, Vice Chancellor, CUTM and Prof. D N Rao, Vice President for giving constant encouragement and support to carry out research at CUTM.

COMPETING INTERESTS

Authors have declared that no competing interests exist.

REFERENCES

1. Cheng KW, Chen YT, Fang WH. Gaussian process regression-based video anomaly detection and localization with hierarchical feature representation. IEEE Transactions on Image Processing. 2015;24(12):5288-5301.
2. Di Mattia F, Galeone P, De Simoni M, Ghelfi E. A survey on gans for anomaly detection. arXiv preprint arXiv:1906.11632; 2019.
3. Reed IS, Yu X. Adaptive multiple-band CFAR detection of an optical pattern with unknown spectral distribution. IEEE Transactions on Acoustics, Speech, and Signal Processing. 1990;38(10):1760-1770.
4. Matteoli S, Diani M, Corsini G. A tutorial overview of anomaly detection in hyperspectral images. IEEE Aerospace and Electronic Systems Magazine. 2010; 25(7):5-28.
5. Banerjee A, Burlina P, Diehl C. A support vector method for anomaly detection in hyperspectral imagery. IEEE Transactions on Geoscience and Remote Sensing. 2006;44(8):2282-2291.
6. Du B, Zhang L. Random-selection-based anomaly detector for hyperspectral imagery. IEEE Transactions on Geoscience and Remote Sensing. 2010; 49(5):1578-1589.
7. Manolakis D, Lockwood R, Cooley T, Jacobson J. Is there a best hyperspectral detection algorithm?. In Algorithms and technologies for multispectral, hyperspectral, and ultraspectral imagery XV. International Society for Optics and Photonics. 2009;7334:733402.
8. Matteoli S, Veracini T, Diani M, Corsini G. Models and methods for automated background density estimation in hyperspectral anomaly detection. IEEE Transactions on Geoscience and Remote Sensing. 2012;51(5):2837-2852.
9. Mahalanobis PC. On the generalized distance in statistics. National Institute of Science of India; 1936.
10. Chang CI, Chiang SS. Anomaly detection and classification for hyperspectral imagery. IEEE Transactions on Geoscience and Remote Sensing. 2002; 40(6):1314-1325.
11. Bhattacharyya A. On a measure of divergence between two statistical populations defined by their probability distributions. Bull. Calcutta Math. Soc. 1943;35:99-109.
12. Sherman S. Solomon Kullback, Information theory and statistics. Bulletin of the American Mathematical Society. 1960; 66(6):472-472.
13. Puzicha J, Hofmann T, Buhmann JM. Non-parametric similarity measures for unsupervised texture segmentation and image retrieval. In Proceedings of IEEE Computer Society Conference on Computer Vision and Pattern Recognition. IEEE. 1997;267-272.
14. Sun W, Du Q. Hyperspectral band selection: A review. IEEE Geoscience and Remote Sensing Magazine. 2019;7(2): 118-139.

15. Küçük S, Yüksel SE. Comparison of RX-based anomaly detectors on synthetic and real hyperspectral data. In 2015 7th Workshop on Hyperspectral Image and Signal Processing: Evolution in Remote Sensing (WHISPERS). IEEE. 2015;1-4.

Peer-review history:
The peer review history for this paper can be accessed here:
https://www.sdiarticle4.com/review-history/73180